

MODELING FINE-SCALE CAPILLARY HETEROGENEITY IN MULTIPHASE FLOW OF CO₂ AND BRINE IN SEDIMENTARY ROCKS

Boxiao Li*, Sally M. Benson* and Hamdi A. Tchelepi*

*Department of Energy Resources Engineering, Stanford University
367 Panama St, Rm 65, Stanford, CA 94305 USA

Key words: Capillary pressure, heterogeneity, simulation, discontinuity, CO₂-brine system, core flood experiment

Summary. Experimental evidence by several groups, including ours, indicates that spatial variations in the capillary-pressure-saturation relationship can dominate the saturation distribution and transport dynamics of CO₂-brine systems in natural porous media. The importance of such small-scale capillary heterogeneity depends strongly on the local balance of the viscous, buoyancy, and capillary forces. In this paper, a numerical scheme suitable for capillary heterogeneity simulations is studied. Several conceptual models, and a CO₂ core flood experiment have been simulated by our in-house simulator. The results are consistent with the theory and experimental observations.

1 INTRODUCTION

Carbon dioxide capture and sequestration (CCS) is believed to be one of the effective ways to reduce anthropogenic CO₂ emission¹. In order to understand the complex physics associated with CO₂ storage, core-scale experiments of CO₂-brine system are performed. Experimental observations from several groups, including ours, show significant spatial variations of the CO₂ saturation in rock cores after CO₂ flooding^{2,3,4}. An example is shown in Figure 1. Spatial heterogeneity in the capillary-pressure-saturation relationship, also called capillary heterogeneity, is believed to be the explanation of this phenomenon^{5,6,7}.

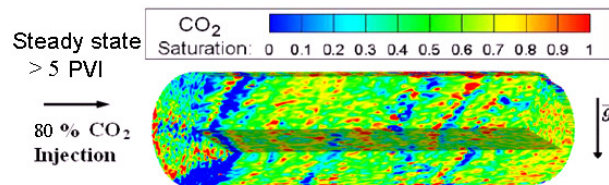


Figure 1: Patchy CO₂ saturation distribution after CO₂ core flooding.

A conceptual description of capillary heterogeneity is as follows. Suppose the flow domain is composed of two contiguous regions, labeled I and II, as shown in Figure 2. The lower capillary-pressure curve corresponds to region I, where the porous medium has a coarse pore structure. Compared with region I, region II has a fine structure, and its capillary-pressure curve is higher. As shown in Figure 2(a), the capillary pressure is continuous across the interface separating the two regions, i.e., $P_c^- = P_c^+$. A pair of distinct saturation values can be found at either side of the interface corresponding to the same capillary pressure. Note that when the capillary pressure of region I is below the entry pressure of region II, there is no corresponding capillary pressure value for region II. In this case, the nonwetting fluid cannot cross the interface, and region II remains fully saturated with the wetting phase.

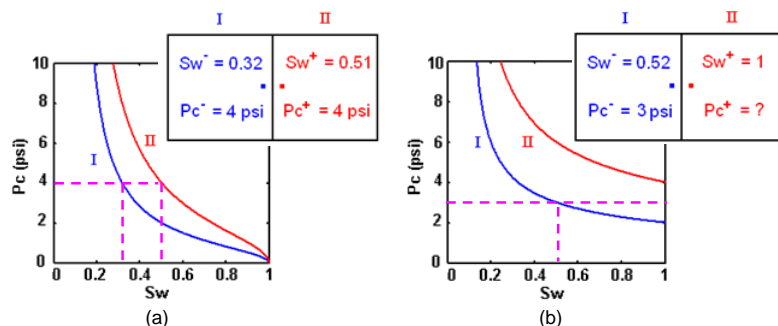


Figure 2: Two types of capillary heterogeneity. (a) Continuous capillarity; (b) Discontinuous capillarity.

In Section 2, a numerical scheme for modeling capillary heterogeneity is described. In Section 3, several simple models are simulated using our in-house simulator, and the results are analyzed. The computational challenges in modeling capillary heterogeneity are also studied. In Section 4, a CO_2 core flood experiment is simulated, and the results are compared with our experimental observations.

2 NUMERICAL SCHEME

Flux continuity of each fluid phase and the correct upstream directions of all phases must be honored in the numerical solutions to ensure local mass conservation^{8,9,10}. Because of spacial variations in the permeability, porosity, and the capillary-pressure-saturation relationship, and the interactions among viscous, buoyancy and capillary forces, the transport dynamics can be very complicated.

2.1 Coupling Flow and Transport

The flow and transport equations can be solved simultaneously (e.g., using Fully Implicit Method, FIM), or sequentially (e.g., using Implicit Pressure Explicit Saturation Method, IMPES, or Sequential Implicit Method, SEQ)¹³. Although SEQ requires less computational effort per timestep than FIM, it is well known that solving the flow and

transport equations separately leads to a mismatch between pressure and saturation. If the flow directions of all the fluid phases remain unchanged during the timestep, such material balance errors are small. These operator-split errors can be further reduced by taking small timestep, or rectified, to some extent, by adding the error back as a source term in the next timestep^{11,12}.

However, the flow direction of a fluid phase may change during a timestep. Such flow reversal is common when gravity segregation or capillary heterogeneity are significant. Hence, when SEQ is used, the upstream direction used in the discrete flow (pressure) equation may be inconsistent with the direction for the transport (saturation) equation. This can cause significant errors in the flux term, leading to convergence problems and possibly wrong solutions, if the saturations at the upstream and downstream side of the gridblock interface are different. This is especially the case when capillary heterogeneity creates a saturation discontinuity across gridblock interfaces. Hence, for SEQ, even though the transport equation is solved implicitly, the timestep has to be small enough to reduce the operator-split error and the effect of flow reversals. For IMPES, capillary heterogeneity creates much more instability than homogeneous capillarity (see Section 3.2 for an example), and thus the timestep has to be very small. To conclude, for capillary heterogeneity problems, the flow and transport equations need to be solved simultaneously. This allows for larger timesteps, while ensuring that the updates of pressure, phase velocities, and saturation are completely consistent with the upstream directions, such that the results ensure local mass conservation of each of the fluid phases.

2.2 Single-Point Phase-Based Upstream Weighting

Due to the hyperbolic character of the governing transport equations, single-point phase-based upstream weighting is widely used¹³. Local mass conservation of discrete approximations is ensured by honoring flux continuity across the control-volume interfaces. When the capillary-pressure-saturation relationship is homogeneous throughout the domain, the saturation distribution is not expected to have local jumps, and the distribution becomes smoother under grid refinement. On the other hand, in the presence of capillary heterogeneity, the saturation distribution is expected to display significant local variations consistent with the capillary-pressure-saturation relation. Single-point, phase-based upstream weighting can resolve the strong discontinuity in saturation and honor flux continuity of each phase by guaranteeing that the flux leaving the upstream gridblock and the flux entering the downstream gridblock are always evaluated using the saturation at their respective upstream side.

Although a variety of different upstream weighting techniques have been proposed to reduce numerical dispersion and grid orientation effects^{14,15}, single-point phase-based upstream weighting is used - almost exclusively - for general-purpose reservoir simulation. In addition, using single-point instead of multi-point upwinding technique is also physically intuitive for capillary heterogeneity problems, because the impact of capillary heterogeneity on flow behavior occurs locally at the interface of rock property discontinuities.

2.3 Assigning Capillary Pressure for Single-Phase Regions

As described in Section 1, when the capillary pressure of a region is below the entry pressure of the adjacent region, capillary pressure is physically undefined in the latter region, where only a single phase (wetting phase) exists. In order to determine the correct phase upstream directions and avoid causing fluid flow that is physically meaningless, we assign a capillary-pressure value for each wetting-phase saturated gridblock, as if an infinitesimal amount of the nonwetting phase exists. This ‘virtual capillary pressure’ equals the entry pressure $P_{c,e}$. An example is provided in Figure 3.

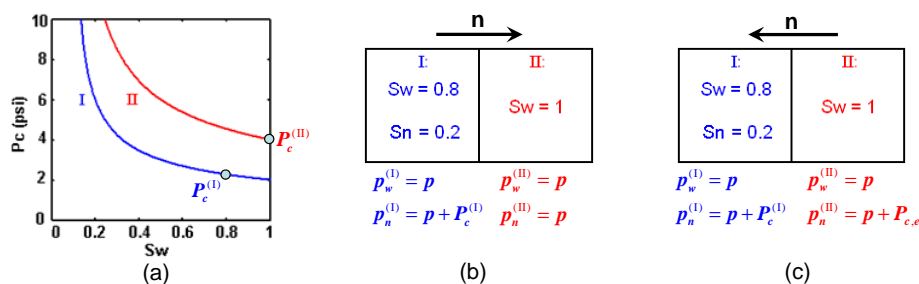


Figure 3: Region II has a higher entry pressure compared to region I. The initial condition is: $S_w^{(I)} = 0.8$, $S_w^{(II)} = 1$, and no fluid exchange will take place. If in region II $p_w = p_n = p$, see (b), the nonwetting phase will flow into region II (as indicated by the arrow), which is not physical. By assigning $P_c^{(II)}$ as $P_{c,e}$, see (c), the nonwetting phase potential direction will point to region I. Because single-point upstream weighting is used, the nonwetting phase transmissibility at the interface is zero (since the upstream S_n is zero). No flow will occur, which is consistent with the physics.

This approach does not affect the pressure continuity of the physically connected phase, regardless of the choice for the primary pressure variable. Suppose that the wetting fluid fully saturates a domain that is composed of regions with heterogeneous capillary entry pressures. Because the nonwetting phase mobility is zero (since $S_n = 0$ everywhere), the mass conservation equations of the wetting and the virtual ‘nonwetting’ phase are reduced to one of the following Laplace equations:

$$\nabla(\lambda_w \nabla p_w) = 0 \quad p_w \text{ as primary pressure variable,} \quad (1)$$

$$\nabla(\lambda_w \nabla (p_n - P_{c,e})) = 0 \quad p_n \text{ as primary pressure variable,} \quad (2)$$

depending on which primary pressure variable is used. The solution of this elliptic equation guarantees that the p_w term in Equation (1), or the $p_n - P_{c,e}$ term in Equation (2) will always be continuous. This suggests that the connected (wetting) phase always has a continuous pressure field. Thus, either the wetting or the nonwetting phase pressure can be used as the primary pressure variable, even if one phase is absent.

3 SIMULATION OF CONCEPTUAL MODELS

3.1 Capillary Equilibrium

The example considers immiscible and incompressible two-phase flow in a 1D horizontal domain, which is composed of two regions of porous media with identical length, but different rock properties. Initially, the left side (region I) is fully saturated with the wetting fluid, and the right side (region II) is fully saturated with the nonwetting fluid. The domain is incompressible with no sources or sinks, and therefore the flow is completely driven by capillary forces. All related properties are listed in Table 1. The capillary-pressure curves for regions I and II are derived using the Leverett J-function based on their porosities and permeabilities.

Table 1: Properties used in capillary equilibrium study.

Porosity	$\phi^{(I)} = \phi^{(II)}$
Permeability	$k^{(I)}/k^{(II)} = 4$
Fluid properties	$\mu_w = \mu_{nw}, \rho_w = \rho_{nw}$
Relative permeability	$k_{rw} = S_w^4, k_{rnw} = (1 - S_w)^2(1 - S_w^2)$
Capillary pressure	$J(S_w) = S_w^{-0.5}, P_c = \sigma \cos \theta \sqrt{\phi/k} \cdot J(S_w)$
Entry pressure ratio	$P_{c,e}^{(I)}/P_{c,e}^{(II)} = 1/2$

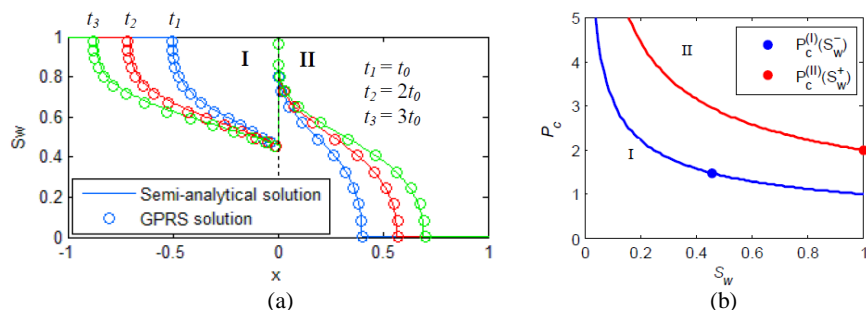


Figure 4: (a) Semi-analytical solution and simulation results. The coordinate is expressed in dimensionless form. (b) Capillary pressure at both sides of the interface.

Van Duijn and de Neef (1996) derived a semi-analytical solution for this problem⁸, which is plotted in Figure 4(a). The saturation values on either side of the region interface are shown in Figure 4(b). As can be seen, the capillary pressure is discontinuous across the interface. Simulation was performed using Stanford General Purpose Research Simulator (GPRS)^{16,17}, and the domain was discretized into 300 gridblocks. The results, shown in Figure 4(a), are in good agreement with the semi-analytical solutions, indicating that flux continuity is honored and that the correct flow directions are computed.

3.2 Capillary vs. Viscous Forces

We now analyze a water-displacing-oil process in a 1D water-wet heterogeneous reservoir core. The core size is $12 \times 5 \times 5 \text{ cm}^3$ and is discretized into 40 gridblocks in the x direction. For each gridblock, the porosity is 0.25, and the permeability follows a lognormal distribution with a mean value of 100 md and a variance of 2500 md^2 . The viscosities, relative permeability curves and the J-function are the same as those in Table 1. Two flow rates are simulated, such that the capillary number $\frac{u\mu_w}{\sigma}$ is on the order of 10^{-7} and 10^{-6} , respectively.

GPRS simulation result at 100 pore volumes injected (PVI) is shown in Figure 5(a). Where there is a fine pore structure (indicated by low permeability), the water saturation tends to be high. The variation of saturation is less for the larger rate, i.e., when viscous force becomes greater. The Courant-Friedrichs-Lewy (CFL) number¹⁸ divided by timestep size (dt) is plotted in Figure 5(b) and compared with the simulation results that use a single homogeneous capillary pressure curve (the average of all the curves). As the figure indicates, when the flow rate is low, the CFL/ dt in the capillary heterogeneity case can be much larger than the homogeneous case. Thus, the combination of dominance of capillarity over the viscous forces and heterogeneous capillarity-pressure-saturation relationships makes the problem more challenging to solve numerically.

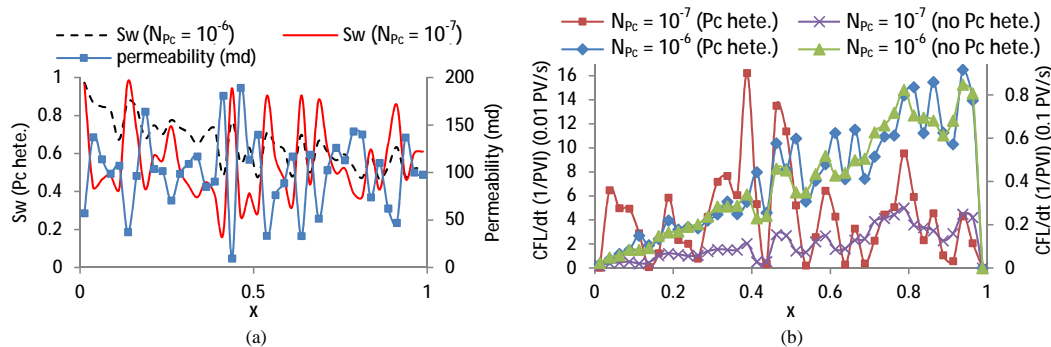


Figure 5: (a) Simulation result at 100 PVI and permeability distribution. (b) CFL/ dt with and without modeling capillary heterogeneity.

4 SIMULATION OF CO_2 CORE FLOOD EXPERIMENT

4.1 Motivations

The migration of CO_2 plumes in storage formations depends strongly on the interaction between viscous, gravity and capillary forces. In order to simulate long-term CO_2 geological storage, the accuracy and efficiency of the numerical simulator in modeling such interactions must be demonstrated. Core flood experiments provide an excellent opportunity to gain deeper understanding of multiphase flow dynamics under controlled

laboratory conditions, and they also serve as a reference for any proposed mathematical model and numerical solution. The in-situ pressure and saturation distributions in the rock are measured using sensors and tomography, allowing direct verification of the simulation results.

4.2 Experiment and Simulation Results

The Berea sandstone core used in the core flood experiment was 5.08 cm in diameter, and 10.2 cm in length. The system was pressurized to 1800 psi and heated to 50 °C. The injection rate was 3 ml/min, with 90 % fractional flow of CO₂. The outlet pressure was kept constant at 1800 psi. The details of the experimental procedure are described by Perrin and Benson (2009)². The laboratory-measured porosity distribution, relative permeability and J-function curves, and the estimated permeability distribution (using the method proposed by Krause et al., 2011)⁵ serve as the input for the GPRS simulator. The simulation results after reaching steady state are compared with the experimental Computerized Tomography (CT) measurements in Figure 6. The computed saturation values agree well with the measured saturations (unit slope in Figure 6). These results indicate that simulations capture the complex pattern of CO₂ distribution, which are highly nonlinear functions of the interactions between capillary heterogeneity, gravity, and viscous forces.

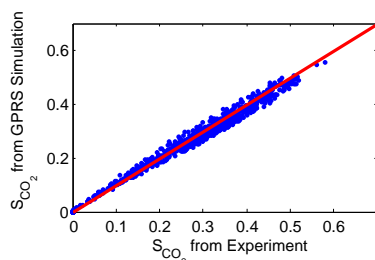


Figure 6: Correlation between experimental measurements and simulation.

5 CONCLUSION

To simulate capillary heterogeneity accurately, flux continuity and correct upstream directions of the two immiscible phases across the interfaces of the control volumes should be honored. Capillary heterogeneity complicates the dynamics and can lead to numerical challenges. Implicit coupling of the flow and transport equations is required, such that the updates of pressure and saturation are completely consistent with the upstream directions of each phase across each control-volume interface. The commonly used single-point phase-based upstream weighting scheme can resolve the discontinuous saturations created by capillary heterogeneity. Although the capillary pressure is physically undefined in regions that are fully saturated by the wetting phase, a capillary pressure value that

corresponds to having an infinitesimal amount of the absent phase should be assigned. This approach will avoid unphysical flow when phase-based single-point upstream weighting is used. A CO₂ core flood experiment have been simulated by our in-house simulator GPRS, and the results are consistent with the experimental observations.

References

- [1] Intergovernmental Panel on Climate Change, *IPCC Special Report on Carbon Dioxide Capture and Storage*, New York: Cambridge University Press, (2005).
- [2] J.C. Perrin and S.M. Benson. An Experimental Study on the Influence of Sub-Core Scale Heterogeneities on CO₂ Distribution in Reservoir Rocks, *Transport in Porous Media*, **82**, 93–109, (2009).
- [3] R. Pini, S.C.M. Krevor, and S.M. Benson. Capillary Pressure and Heterogeneity for the CO₂/Water System in Sandstone Rocks at Reservoir Conditions, *Advances in Water Resources*, **38**, 48–59, (2012).
- [4] J.Q. Shi, Z. Xue and S. Durucana. Supercritical CO₂ Core Flooding and Imbibition in Tako Sandstone: Influence of Sub-Core Scale Heterogeneity, *International Journal of Greenhouse Gas Control*, **5**, 75–87, (2011).
- [5] M.H. Krause, J.C. Perrin, and S.M. Benson. Modeling Permeability Distributions in a Sandstone Core for History Matching Coreflood Experiments, *SPE Journal*, **16**, 768–777, (2011).
- [6] C.W. Kuo, J.C. Perrin and S.M. Benson. Effect of Gravity, Flow Rate, and Small Scale Heterogeneity on Multiphase Flow of CO₂ and Brine, paper SPE 132607, (2010).
- [7] S.C.M. Krevor, R. Pini, B. Li, and S.M. Benson. Capillary Heterogeneity Trapping of CO₂ in a Sandstone Rock at Reservoir Conditions, *Geophysical Research Letters*, **38**, L15401, (2011).
- [8] C.J. van Duijn and M.J. de Neef. Self-Similar Profiles for Capillary Diffusion Driven Flow in Heterogeneous Porous Media, *Centrum voor Wiskunde en Informatica Report*, AM-R9601, (1996).
- [9] C. Cancès. Finite Volume Scheme for Two-Phase Flows in Heterogeneous Porous Media Involving Capillary Pressure Discontinuities, *ESAIM: Mathematical Modelling and Numerical Analysis*, **43**, 973–1001, (2009).
- [10] F. Kwok and H.A. Tchelepi. Potential-Based Reduced Newton Algorithm for Nonlinear Multiphase Flow in Porous Media, *Journal of Computational Physics*, **227**, 706–727, (2007).
- [11] A.G. Spillette, J.G. Hillestad and H.L. Stone. A High-Stability Sequential Solution Approach to Reservoir Simulation, paper SPE 4542, (1973).
- [12] J.W. Watts. A Compositional Formulation of the Pressure and Saturation Equations, *SPE Reservoir Engineering*, May, 243–252, (1986).
- [13] K. Aziz and A. Settari. *Petroleum Reservoir Simulation*, Applied Science Publishers, London, England, (1979).
- [14] M.R. Todd, P.M. O’Dell and G.J. Hirasaki. Methods for Increased Accuracy in Numerical Reservoir Simulators, paper SPE 3516, (1972).
- [15] J. Kozdon, B. Mallison, M. Gerritsen and W. Chen. Multidimensional Upwinding for Multiphase Transport in Porous Media, *SPE Journal*, **16**, 263–272, (2011).
- [16] H. Cao. *Development of Techniques for General Purpose Simulators*, PhD thesis, Stanford University, (2002).
- [17] Y. Jiang. *Techniques for Modeling Complex Reservoirs and Advanced Wells*, PhD thesis, Stanford University, (2007).
- [18] K.H. Coats. IMPES Stability: Selection of Stable Timesteps, *SPE Journal*, June, 181–187, (2003).